

Altuntaş et al., 2023

Volume 9, pp. 113-126

Received: 19th June 2023

Revised: 29th June 2023, 12th October 2023, 25th October 2023

Accepted: 31st October 2023

Date of Publication: 15th November 2023

DOI- <https://doi.org/10.20319/mijst.2023.9.113-126>

This paper can be cited as: Altuntaş, G., Altuntaş, O. & Bostan, B. (2023). Effect of Cryogenic and Natural Aging Process Applied to Al-Zn-Mg-Cu Alloys on Life Time Calculation. MATTER: International Journal of Science and Technology, 9, 113-126.

This work is licensed under the Creative Commons Attribution-Non-commercial 4.0 International License. To view a copy of this license, visit <http://creativecommons.org/licenses/by-nc/4.0/> or send a letter to Creative Commons, PO Box 1866, Mountain View, CA 94042, USA.

EFFECT OF CRYOGENIC AND NATURAL AGING PROCESS APPLIED TO Al-Zn-Mg-Cu ALLOYS ON LIFE TIME CALCULATION

Gözde Altuntaş

*Faculty of Technology, Department of Metallurgical and Materials Engineering, Gazi
University, Ankara, Turkey*
gozdealtuntas@gazi.edu.tr

Onur Altuntaş

*Department of Warfare Weapons and Tools, Alparslan Defense Sciences and National Security
Institute, National Defense University, Ankara, Turkey*
oaltuntas@kho.msu.edu.tr

Bülent Bostan

*Faculty of Technology, Department of Metallurgical and Materials Engineering, Gazi
University, Ankara, Turkey*
bostan@gazi.edu.tr

Abstract

In this study, life time calculation of aluminum 7075 alloy with cryogenic and natural aging processes was performed by thermal analysis. The aluminum alloy was quenched after solid solution treatment at 480°C and naturally aged for 10-100 days at room temperature (25°C). Other samples were cryogenically treated at -40°C and -80°C for 2 hours after solid solution

treatment at 480°C. After the cryogenic treatment, natural aging was done at room temperature for 10-100 days. At the end of each period determined for the samples, the hardness values were measured. It was observed that there was no significant change in hardness values at the end of 10 and 100 days at -80 °C. Thus, it was determined that the natural aging process does not start after cryogenic treatment at -80 °C. It was observed that the hardness value of naturally aged samples after cryogenic treatment at -40 °C increased more than the natural aged samples only. This showed that -40 °C improved the mechanism by creating a driving force in the material. Life time calculations between 30 °C and 320 °C also showed that -40 °C cryogenic treatment + natural aging increased life time by approximately 20% compared to natural aging alone.

Keywords

Al-Zn-Mg-Cu Alloy, Cryogenic Treatment, Natural Aging, Life Time Calculation

1. Introduction

Al-Zn-Mg-Cu alloys are also included in the 7xxx series aluminum alloys group. Due to its features such as low density and high strength, it is frequently preferred in structural applications and in the aviation industry. Since this alloy is in the group of aging aluminum alloys, it is often used by applying aging heat treatment (Altuntas et al., 2022). Thanks to this heat treatment, the strength ratio increases and a wide usage area is formed (Chen et al., 2009). The aging heat treatment is divided into two groups artificial and natural. With natural aging; Depending on the ratio of chemical elements, the solution heat treatment is carried out for 1 or 2 hours at (400-500°C) in general, water is given and a supersaturated solid solution is formed (Altuntas et al., 2021).

The main purpose of the solid solution heat treatment is to increase the solubility of the alloy by heating to a high temperature, to dissolve the precipitates in the structure in a single phase, and to obtain a supersaturated single-phase solid solution. If the alloy is allowed to cool slowly after solution treatment, coarse precipitates with negative mechanical properties are formed. As a result of rapid quenching, a supersaturated α -phase precipitate is obtained by not allowing the second phase to precipitate in the α solid. The α -phase is unstable due to the effect of flash cooling.

The number of atomic cavities in equilibrium in the alloy increases logarithmically with the increase in temperature. The volume fraction of atomic vacancies during the solution process is quite high compared to their ratio at low temperatures. In this case, as the equilibrium conditions

cannot be achieved as a result of the sudden cooling of the material from high temperatures, the excess of atomic vacancies remains in the structure. Atomic cavities, which are found in large amounts in the structure, are formed as a result of sudden cooling and move away from the structure over time. Atomic cavities that form point defects tend to come together and coalesce, and some of them absorb the atomic cavities and form the basis for the formation of dislocation rings. During quenching, the solid solution becomes unstable and tends to precipitate. It is then left to natural aging by keeping it at room temperature (Mackenzie et al., 2003). It takes about six months to achieve maximum hardness with this process (Mukhopadhyay et al., 2011).

Artificial aging heat treatment, on the other hand, is carried out by giving water (80°C-200°C) after the solution heat treatment (holding for 1 or 2 hours between 400-500°C) and keeping the material for 12-24 hours. The aging time varies according to the temperature. By keeping the rapidly cooled alloy at a temperature above room temperature, precipitation takes place in a shorter time due to the increased diffusion rate. With both aging, the same phase occurs, which increases the strength of the material. In practice, artificial aging is frequently used to save time. But during natural aging, not only the size and number density, but also the type of clusters and GP zones can change over time, and this can have a profound effect on the metastable η' phase. It has been observed in different studies that the microstructural evolution and the form of the formed phases during natural aging have a deeper effect (Liu et al., 2015). The precipitation sequences formed during aging of Al-Zn-Mg-Cu alloys have been shown in many studies (Sha et al., 2004). It is well known that Guinier-Preston (GP) zones with hardening effect and metastable η' phase precipitates can form from supersaturated solid solution during aging (SSSS) (Couturier et al., 2017). In general, there are two types of GP zones. These are GPI zones and GPII zones. The sequences shown below are most likely to arise during aging.

SSSS \rightarrow GPI zones \rightarrow GP II zones \rightarrow Metastable η' (MgZn_2) \rightarrow Stable η (MgZn_2)
consists of sequentially (Lendvai, 1996).

It has been reported that the effect on the highest strength increase is associated with the metastable η' phase (Li et al., 1999). The precipitation kinetics of the formation of this phase has been investigated in different studies (Khalfallah, et al., 2019). Thus, the activation energies, growth and nucleation kinetics of the phases are shown. The precipitate kinetics of the phases after secondary treatments were also investigated in different studies (Leyva-González et al., 2015). However, there are no studies on the precipitate kinetics and life time calculation of the η' phase

after natural aging. With this study, information about the degradation time of the material depending on the temperature will be obtained through thermal analysis, especially with life time calculation in all material groups.

2. Experimental Studies

The Al 7075 alloy used in this study was purchased commercially. Solution heat treatment of samples cut in 10*10*10 mm³ dimensions was first performed in high temperature furnace at 480 °C for 2 hours. Then it was quenched and some of the samples were left to natural aging for 10 and 100 days at room temperature. These samples were coded as NA10 and NA100, respectively. Other cut samples were cryogenically treated at -40 °C and -80 °C for 2 hours after solution heat treatment and quenching. Then it was left to natural aging for 10 and 100 days. After each aging period, the mechanical change was controlled by measuring their microhardness.

However, there was no change in the mechanical hardness values of the samples that were cryogenically treated at -80 °C during this period. This showed that the aging mechanism could not start after cryogenic treatment at -80 °C. Therefore, these samples were not coded. Due to the effective initiation of natural aging after cryogenic treatment at -40 °C, these samples were coded as CNA10 and CNA100, respectively. Hardness measurements were taken in the Qness hardness device according to the ASTM E384 standard. HITACHI DSC 7020 thermal analyzer was used for differential scanning calorimetry (DSC) experiments. The tests were carried out at a temperature range of 30 °C to 320 °C in an argon atmosphere with a heating rate of 5 °C /min, 10 °C /min, 15 °C /min, and 20 °C/min. DSC analysis was carried out with samples of 10 mg mass enclosed in aluminum pans. With the data obtained through this analysis, first of all, the activation energies were found and a lifetime calculation was made.

Table 1: *Chemical Composition of the Material*

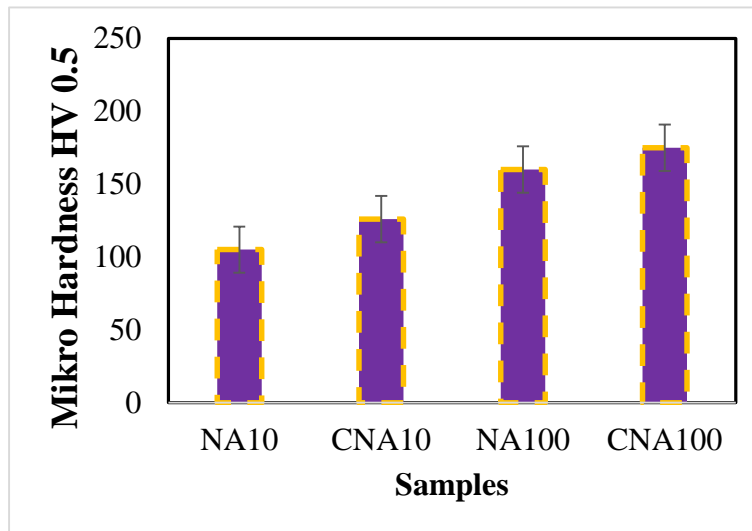
Elements (%)						
Zn	Mg	Cu	Mn	Cr	Fe	Al
5.9	2.7	1.8	0.3	0.25	0.4	Balance

(Source: Seykoc Aluminum Company)

3. Result and Discussion

Figure 1 shows the micro hardness values of the samples. The hardness of the NA10 sample was measured as 105 HV0.5, and the hardness of the NA100 sample was measured as 160 HV0.5. It was observed that the hardness value of the material increased as the natural aging time increased. This is an expected result as observed in the literature (Altuntaş et al., 2022). When we look at the hardness value after cryogenic treatment at $-80\text{ }^{\circ}\text{C}$ and 10 days of natural aging, the hardness value was measured as 100 HV0.5. After 100 days, the hardness value was measured as 108 HV0.5. It has been observed that the cryogenic process performed at $-80\text{ }^{\circ}\text{C}$ has a bad effect on the progression of natural aging. For this reason, life time calculations of the experiments carried out at $-80\text{ }^{\circ}\text{C}$ were not performed. After the cryogenic treatment at $-40\text{ }^{\circ}\text{C}$ and 10 days of natural aging, the hardness of the CNA10 sample was measured at 126 HV0.5. The hardness value after 100 days of natural aging was found to be 175 HV0.5. The results showed that cryogenic treatment at $-40\text{ }^{\circ}\text{C}$ is an effective force in accelerating the aging mechanism. It is thought that the probability of the formation of more η' phases by triggering the formation of new nucleation points will increase the hardness.

Figure 1: Micro Hardness Values of Samples According to HV0.5



(Source: Author's Own Illustration)

As seen in Figure 2, the activation energy graph is shown with the data obtained as a result of the DSC analyzes performed in an argon atmosphere with a heating rate of $5\text{ }^{\circ}\text{C} / \text{min}$, $10\text{ }^{\circ}\text{C} / \text{min}$, $15\text{ }^{\circ}\text{C} / \text{min}$, $20\text{ }^{\circ}\text{C} / \text{min}$. Table 2 shows the life time calculation of the NA10 sample between 30

°C and 320 °C. In general, it was observed that the life time value decreased as the temperature increased.

Conventionally, the reaction rate is calculated according to the Arrhenius equation.

$$\frac{dx}{dt} = A \exp\left(-\frac{\Delta E}{RT}\right) \cdot f(x)$$

$$\int_{x_0}^{x_1} \frac{dx}{f(x)} = \int_{t_0}^{t_1} A \exp\left(-\frac{\Delta E}{RT}\right) dt$$

$$= \frac{A}{B} \int_{T_0}^{T_1} \exp\left(p - \frac{\Delta E}{RT}\right) dT$$

So, if F(x) is defined as:

$$F(x) = \int \frac{dx}{f(x)}$$

and after changing the following variables, integration is performed according to the parts.

$$\frac{\Delta E}{RT} = y$$

$$F(x_1) - F(x_0) = A \frac{\Delta E}{BR} \left[P\left(\frac{\Delta E}{RT_1}\right) - P\left(\frac{\Delta E}{RT_0}\right) \right] \dots\dots\dots$$

$$P(y) = \frac{e^{-y}}{y} - \int_y^\infty \frac{e^{-y}}{y} dy$$

$$\frac{A \cdot \Delta E}{BR} P\left(\frac{\Delta E}{RT_1}\right) = F(x_1) - F(x_0) \dots\dots\dots$$

$$\frac{A \cdot \Delta E}{BR} P\left(\frac{\Delta E}{RT_1}\right) = \text{const.}$$

$$\text{Log}P(y) = 2.315 - 0.467y \quad 20 < y < 60$$

$$\text{Const} = \log \frac{A \cdot \Delta E}{BR} P\left(\frac{\Delta E}{RT_1}\right)$$

$$= \log \frac{A \cdot \Delta E}{BR} + \log P\left(\frac{\Delta E}{RT_1}\right)$$

$$= \log \frac{A \cdot \Delta E}{BR} - \log B - 2.315 - 0.467 \left(\frac{\Delta E}{RT_1}\right)$$

$$\log B = -0.467 \frac{\Delta E}{R} * \frac{1}{T_1} + \text{constant}$$

$$\Delta E_i = -\frac{R}{0.4567} * q_i \text{ (kj/mol) } R=8.31434 \text{ (kj/mol)}$$

The constant temperature degradation time (τ) is calculated as

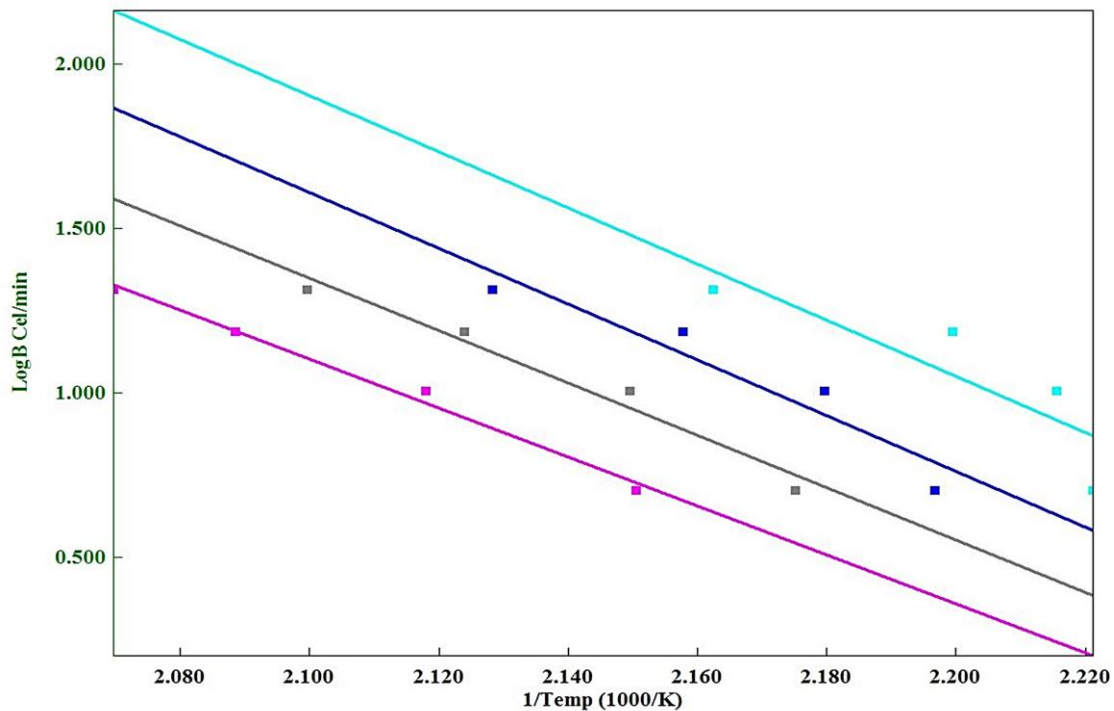
The temperature to be kept is considered as T_c ($^{\circ}\text{C}$).

$$B = \sqrt{\max B_j * \min B_j} \text{ (use midpoint of } \log B)$$

$$T_i = -\frac{q_i}{\log B - P_i} \text{ (K)}$$

$$\tau_i = \frac{\int_{T_0}^{T_i} \exp\left(-\frac{\Delta E}{RT}\right) dT}{B \exp\left(-\frac{\Delta E_i}{R(T_c + 273.15)}\right)}$$

Figure 2: Activation Energy Graph of NA10 Sample



(Source: Author's Own Illustration)

Table 2: Life Time Calculation and Activation Energy Values of NA10 Sample in the Range Of 30-320 °C

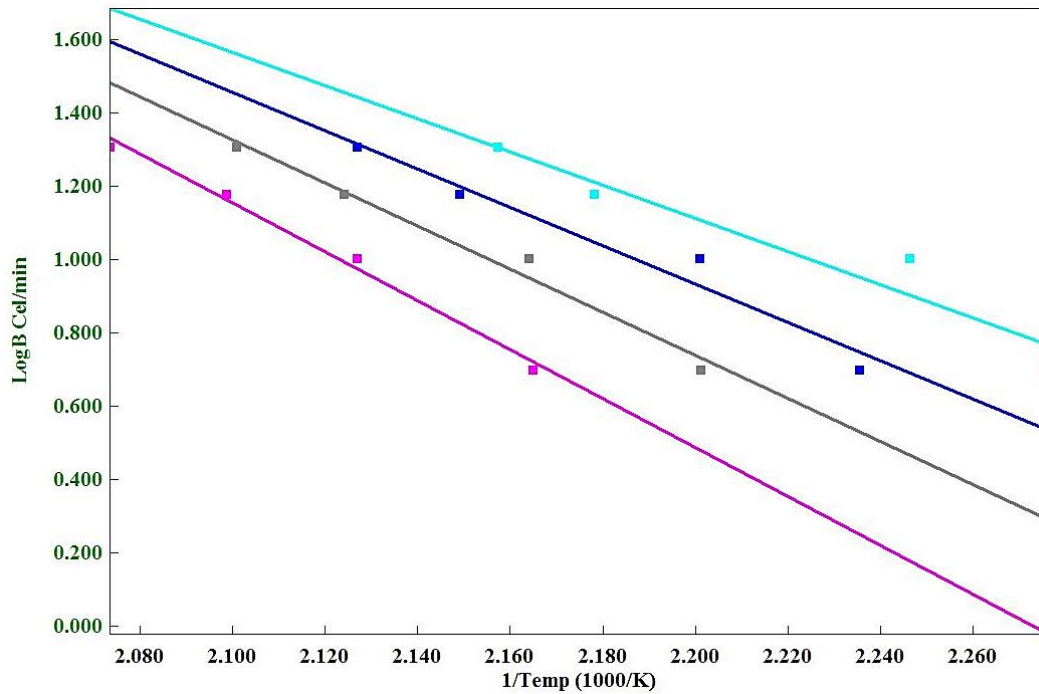
Life Time						
R.F %	ΔE kJ/mol	30 °C day	40 °C day	50 °C day	60 °C day	70 °C day
20	97	3.6E+02	1.1E+02	3.3E+01	1.1E+01	4.1E+00
40	105	1.6+E+03	4.1E+02	1.2E+02	3.7E+01	1.2E+01
60	111	5.5+03	1.3E+03	3.6E+02	1.0E+02	3.2E+01
80	118	2.1+04	4.7E+03	1.2E+03	3.1E+02	8.9E+01
Life Time						
R.F %	ΔE kJ/mol	80 °C day	90 °C day	100 °C day	110 °C day	120 °C day
20	97	1.6E+00	6.2E-01	2.6E-01	1.2E-01	5.4E-02
40	105	4.3E+01	1.6E+00	6.3E-01	2.6E-01	1.1E-01
60	111	1.0E+01	3.6E+00	1.4E+00	5.3E-01	2.2E-01
80	118	2.7E+01	9.0E+00	3.2E+00	1.2E+00	4.5E-01
Life Time						
R.F %	ΔE kJ/mol	130 °C day	140 °C day	150 °C day	160 °C day	170 °C day
20	97	2.6E-02	1.3E-02	6.6E-03	3.5E-03	1.9E-03
40	105	5.0E-02	2.4E-02	1.1E-02	5.7E-03	3.0E-03
60	111	9.3E-02	4.1E-02	1.9E-02	9.2E-03	4.6E-03
80	118	1.9E-01	7.9E-02	3.5E-02	1.6E-02	7.6E-03
Life Time						
R.F %	ΔE kJ/mol	180 °C day	190 °C day	200 °C day	210 °C day	220 °C day
20	97	1.1E-03	6.1E-04	3.6E-04	2.1E-04	1.3E-04
40	105	1.6E-03	8.6E-04	4.8E-04	2.8E-04	1.6E-04
60	111	2.3E-03	1.2E-03	4.7E-04	3.7E-04	2.1E-04

80	118	3.8E-03	1.9E-03	1.0E-03	5.3E-04	2.9E-04
Life Time						
R.F %	ΔE kJ/mol	230 °C day	240 °C day	250 °C day	260 °C day	270 °C day
20	97	8.2E-05	5.2E-05	3.4E-05	2.2E-05	1.5E-05
40	105	9.8E-05	6.0E-05	3.8E-05	2.4E-05	1.5E-05
60	111	1.2E-04	7.3E-05	4.4E-05	2.7E-05	1.7E-05
80	118	1.7E-04	9.6E-05	5.6E-05	3.4E-05	2.1E-05
Life Time						
R.F %	ΔE kJ/mol	280 °C day	290 °C day	300 °C day	310 °C day	320 °C day
20	97	1.0E-05	6.9E-06	4.8E-06	3.4E-06	2.4E-06
40	105	1.0E-05	6.8E-06	4.6E-06	3.1E-06	2.2E-06
60	111	1.1E-05	7.1E-06	4.7E-06	3.2E-06	2.1E-06
80	118	1.3E-05	8.1E-06	5.2E-06	3.4E-06	2.3E-06

(Source: Author's Own Illustration)

In Figure 3 and Table 3, activation energy and life time calculation values of the CNA10 sample, which was cryogenically treated and aged for 10 days, are shown. When we look at the values, it has been calculated that natural aging after cryogenic treatment at -40 °C increases the hardness and has a positive effect on life time. Up to 180 °C, the life time value of the CNA10 sample increased compared to the NA10 sample. In other words, the formation of more nucleation points by cryogenic treatment represents the formation of more η' phase, supporting the increase in life time value. It is thought that the degradation time of the η' phase, that is, the decrease in the life time value in the CNA10 sample after 180 °C, may have entered the extreme aging phase after this temperature (Wang et al., 2022). Formation of more η' phases by cryogenic treatment will require further reduction as degradation occurs or as overaging occurs. For this reason, there may be a greater decrease in the life time value compared to the NA10 sample.

Figure 3: Activation Energy Graph of CNA10 Sample



(Source: Author's Own Illustration)

Table 3: Life time calculation and activation energy values of CNA10 sample in the range of 30-320 °C

Life Time						
R.F %	ΔE kJ/mol	30 °C day	40 °C day	50 °C day	60 °C day	70 °C day
20	110	1.2E+02	3.2E+02	8.6E+01	2.5E+01	7.7E+00
40	114	3.7E+03	8.6E+02	2.2E+02	6.2E+01	1.8E+01
60	115	7.2+03	1.7E+03	4.2E+02	1.2E+02	3.4E+01
80	116	1.5+04	3.3E+03	8.3E+02	2.2E+02	6.5E+01
Life Time						
R.F %	ΔE kJ/mol	80 °C day	90 °C day	100 °C day	110 °C day	120 °C day
20	110	6.6E+00	9.1E-01	3.4E-01	1.3E-01	5.5E-02
40	114	5.9E+01	2.0E+00	7.4E-01	2.8E-01	1.1E-01
60	115	1.1E+01	3.7E+00	1.8E+00	5.0E-01	2.0E-01

80	116	2.0E+01	6.8E+00	2.4E+00	9.1E-01	3.6E-01
Life Time						
R.F %	ΔE kJ/mol	130 °C day	140 °C day	150 °C day	160 °C day	170 °C day
20	110	2.8E-02	1.3E-02	4.9E-03	3.7E-03	1.2E-03
40	114	5.2E-02	2.5E-02	9.4E-02	5.8E-03	3.1E-03
60	115	9.4E-02	4.2E-02	1.9E-02	7.6E-03	4.8E-03
80	116	2.0E-01	8.1E-02	3.6E-02	1.7E-02	7.7E-03
Life Time						
R.F %	ΔE kJ/mol	180 °C day	190 °C day	200 °C day	210 °C day	220 °C day
20	110	6.1E-04	3.2E-04	1.8E-04	9.8E-05	5.6E-05
40	114	1.7E-03	5.7E-04	3.0E-04	1.7E-04	9.3E-05
60	115	2.6E-03	9.5E-03	5.0E-04	2.7E-04	1.5E-04
80	116	3.8E-03	1.6E-03	8.4E-04	4.6E-04	2.5E-04
Life Time						
R.F %	ΔE kJ/mol	230 °C day	240 °C day	250 °C day	260 °C day	270 °C day
20	110	3.3E-05	1.9E-05	1.2E-05	7.3E-06	4.6E-06
40	114	5.4E-05	3.1E-05	1.9E-05	1.1E-05	7.2E-06
60	115	8.7E-05	5.1E-05	3.0E-05	1.1E-05	1.1E-05
80	116	1.4E-04	8.3E-05	4.9E-05	3.0E-05	1.8E-05
Life Time						
R.F %	ΔE kJ/mol	280 °C day	290 °C day	300 °C day	310 °C day	320 °C day
20	110	3.0E-06	1.9E-06	1.3E-06	8.6E-07	5.8E-07
40	114	4.5E-06	2.9E-06	1.9E-06	1.3E-06	8.5E-07
60	115	7.2E-06	4.6E-06	3.0E-06	2.0E-06	1.3E-06
80	116	1.1E-05	7.3E-06	4.7E-06	3.1E-06	2.1E-06

(Source: Author's Own Illustration)

4. Conclusions

In this study, the effect of natural aging and cryogenic treatment on life time calculation of 7075 Al alloy was investigated. The data obtained as a result of experiments and calculations are as follows.

- It has been determined that natural aging does not start after cryogenic treatment at -80°C.
- After cryogenic treatment at -40 °C, the hardness value of naturally aged samples increased by 10% compared to only naturally aged samples.
- -40 °C cryogenic treatment + natural aging increased lifetime by approximately 20% compared to natural aging alone.

4.1. Scope of Future Research and Research Limitations

This study will provide an infrastructure that can be studied in detail in a different material group with this method in future research.

ACKNOWLEDGMENTS

This study has been financially supported by the Gazi University Scientific Research Projects Coordination Unit [under Project Number FDK-2023-7620].

CONFLICT OF INTEREST

There is no conflict of interest between the authors.

REFERENCES

- Altuntaş, G., Altuntaş, O., & Bostan, B. (2021). Characterization of Al-7075/T651 Alloy by RRA Heat Treatment and Different Pre-deformation Effects. Transactions of the Indian Institute of Metals, 74, 3025-3033. <https://doi.org/10.1007/s12666-021-02369-5>
- Altuntaş, G., Bostan, B. (2022). Metallurgical characterization of natural aging effects on pre-deformed Al 7075/T651 alloy during retrogression and re-aging heat treatment. Kovove Materialy, 60(4) <https://doi.org/10.31577/km.2022.4.209>
- Altuntaş, G., & Bostan, B. (2021). Al-Zn-Mg-Cu Alaşımının Kristalografisine RRA Isıl İşlemi Etkilerinin İncelenmesi. Politeknik Dergisi, 25(2), 871-877. <https://doi.org/10.2339/politeknik.919492>

- Altuntaş, G., & Bostan, B. (2022) 7075 Al Alaşımına Uygulanan Kriyojenik ve Doğal Yaşlandırma İşleminin Avrami Parametresine Etkisi. *Gazi University Journal of Science Part C: Design and Technology*, 10(4), 691-698.
<https://doi.org/10.29109/gujsc.1179514>
- Chen, J., Zhen, L., Yang, S., Shao, W., & Dai, S. (2009). Investigation of precipitation behavior and related hardening in AA 7055 aluminum alloy. *Materials Science and Engineering: A*, 500(1-2), 34-42. <https://doi.org/10.1016/j.msea.2008.09.065>
- Couturier, L., Deschamps, A., De Geuser, F., Fazeli, F., & Poole, W. J. (2017). An investigation of the strain dependence of dynamic precipitation in an Al-Zn-Mg-Cu alloy. *Scripta Materialia*, 136, 120-123. <https://doi.org/10.1016/j.scriptamat.2017.04.031>
- Khalfallah, A., Raho, A. A., Amzert, S., & Djemli, A. (2019). Precipitation kinetics of GP zones, metastable η' phase, and equilibrium η phase in Al– 5.46 wt. % Zn– 1.67 wt. % Mg alloy. *Transactions of Nonferrous Metals Society of China*, 29(2), 233-241.
[https://doi.org/10.1016/S1003-6326\(19\)64932-0](https://doi.org/10.1016/S1003-6326(19)64932-0)
- Lendvai, J. (1996). Precipitation and strengthening in aluminum alloys. In *Materials Science Forum* (Vol. 217, pp. 43-56). Trans Tech Publications Ltd.
<https://doi.org/10.4028/www.scientific.net/MSF.217-222.43>
- Leyva-González, K. A., Deaquino-Lara, R., Pourjafari, D., Martínez-Sánchez, R., Hernandez-Rodriguez, M. A. L., & García-Sánchez, E. (2015). Calorimetry study of the precipitation in an Al7075-graphite composite fabricated by mechanical alloying and hot extrusion. *Journal of Thermal Analysis and Calorimetry*, 121, 589-595.
<https://doi.org/10.1007/s10973-015-4581-5>
- Li, X. Z., Hansen, V., Gjønnes, J., & Wallenberg, L. R. (1999). HREM study and structure modeling of the η' phase, the hardening precipitates in commercial Al–Zn–Mg alloys. *Acta materialia*, 47(9), 2651-2659. [https://doi.org/10.1016/S1359-6454\(99\)00138-X](https://doi.org/10.1016/S1359-6454(99)00138-X)
- Liu, S., Li, C., Han, S., Deng, Y., & Zhang, X. (2015). Effect of natural aging on quench-induced inhomogeneity of microstructure and hardness in high strength 7055 aluminum alloy. *Journal of alloys and compounds*, 625, 34-43.
<https://doi.org/10.1016/j.jallcom.2014.10.195>
- Mackenzie, D. S., & Totten, G. E. (Eds.). (2003). *Handbook of aluminum*. New York: Dekker.
<https://doi.org/10.1201/9780429223259-10>

Mukhopadhyay, A. K., & Prasad, K. S. (2011). Formation of plate-shaped Guinier–Preston zones during natural aging of an Al–Zn–Mg–Cu–Zr alloy. *Philosophical magazine letters*, 91(3),

214-222. <https://doi.org/10.1080/09500839.2010.547525>

Sha, G., & Cerezo, A. (2004). Early-stage precipitation in Al–Zn–Mg–Cu alloy (7050). *Acta materialia*, 52(15), 4503-4516. <https://doi.org/10.1016/j.actamat.2004.06.025>

Wang, J., Chen, X., Yang, L., & Zhang, G. (2022). Effect of preheat & post-weld heat treatment on the microstructure and mechanical properties of 6061-T6 aluminum alloy welded sheets. *Materials Science and Engineering: A*, 841, 143081.

<https://doi.org/10.1016/j.msea.2022.143081>